

On the Structural Stability and Optical Properties of Germanium-based Schwarzites: A Density Functional Theory Investigation

Raphael M. Tromer,[†] Levi C. Felix,^{†,‡} Cristiano F. Woellner,[¶] and Douglas S. Galvao^{*,†}

[†]*Applied Physics Department, State University of Campinas, Campinas, SP, 13083-970, Brazil*

[‡]*Center for Computational Engineering and Sciences, State University of Campinas, Campinas, SP, 13083-970, Brazil*

[¶]*Physics Department, Federal University of Parana, UFPR, Curitiba, PR, 81531-980, Brazil*

E-mail: galvao@ifi.unicamp.br

Abstract

Since graphene was synthesized the interest for building new 2D and 3D structures based on the carbon allotropes has been growing every day. One of these 3D structures is known as carbon schwarzites. Schwarzites consist of carbon nanostructures possessing the shape of Triply-Periodic Minimal Surfaces (TPMS), which is characterized by a negative Gaussian curvature introduced by the presence of carbon rings with more than six atoms. Some examples of schwarzite families include: primitive (P), gyroid (G) and diamond (D). Previous studies considering different element species of schwarzites have investigated the mechanical, electrical and thermal properties. In

this work, we investigated the stability of germanium (Ge) schwarzites using density functional theory with GGA exchange-correlation functional. We chose one structure of each family (P8bal), (G688) and (D688). It was observed that regions usually flat in carbon schwarzites acquires buckled configurations as previously observed on silicene and germanene monolayers. The investigated structures presented a semiconducting bandgap ranging from 0.13 to 0.27 eV. We also performed calculations of optical properties within the linear regime, where it was shown that Ge schwarzites structures absorb light from infrared to ultra-violet frequencies. Therefore, our results open new perspectives of materials that can be used in optoelectronics devices application.

Introduction

Proposed in 1991 by Mackay and Terrones,¹ schwarzites are crystalline structures where triply periodic minimal surfaces (TPMS) are decorated with carbon atoms along their surface. Although schwarzites have not been synthesized yet, they were found to be energetically stable,^{2–5} thus, motivating the recent investigations on possible synthetic routes, such as zeolite templating^{6–8} and multifold C-C coupling reactions.⁹

Theoretical investigations have shown that schwarzites possess unique mechanical properties, such as the ability to be compressed to very high strain values without breaking,^{10–13} high energy-absorption performance,^{12,14} near-zero Poisson’s ratio for most structures^{11,12} and an auxetic behavior (negative Poisson’s ration) only in a range of deformation for some structures.¹² Also, many potential applications have been proposed, such as catalysis, molecular sieving,^{15,16} gas storage,^{17,18} alkali ion batteries,¹⁹ as anode for lithium-ion batteries²⁰ and energy-absorbing materials.^{14,21–24} Different schwarzite structures possess distinct electronic properties, where the bandgap values vary from metallic to semiconductor.^{25–29} Interestingly, first-principles calculations³⁰ predict that some structures can even exhibit Dirac-like points similar to graphene. Schwarzites have also interesting magnetic properties, as some structures were predicted to present a net magnetic moment in their electronic ground

state.³¹ It has also been predicted that the presence of negative Gaussian curvatures can induce suppression in the lattice thermal conductivity,^{32,33} which can be further tuned by the introduction of guest atoms in their pores making them good candidates for thermoelectric applications.³⁴

Despite being originally proposed as carbon-based materials, in principle schwarzites can also be made of other elements and in fact, this has been already investigated. Boron nitride-based (BN) schwarzites were found to be wide bandgap semiconductors or insulators depending on the structure topology.³⁵ Also, hydrides and oxides of boron, carbon, nitrogen, aluminum,³⁶ and silicon³⁷ have been investigated with density functional theory. Silicon (Si) and germanium (Ge) have a stronger sp^3 character than carbon and significant structural differences are expected to occur in many analogs of carbon nanostructures such as closed cage structures,³⁸ nanotubes,^{39–44} and even two-dimensional honeycomb graphene-like sheets,^{45–49} the so-called silicene and germanene, which have already been experimentally realized.^{50–53} More recently, multilayer silicene has been synthesized and shown to be promising for electronic applications⁵⁴ as well as stable under ambient conditions.⁵⁵ These important and significant differences among carbon and silicon and/or germanium structures appear mainly in the form of structural buckling due to the pseudo-JahnTeller effect (PJTE).^{56,57} Structural buckling of both silicene and germanene structures have been already demonstrated.⁴⁶ Due to these differences, unique silicon and germanium structures can exist with no corresponding carbon counterpart.⁵⁸ Based on that it would be interesting to investigate the structural and electronic properties of germanium-based schwarzites. Schwarzite families contain many structures, in the present work we select one representative structure of the primitive (P8bal), gyroid (G688), and diamond (D688) families (see Figure 1).

Materials and Methods

In order to investigate the structural stability of germanium schwarzites, we used first-principles calculations based on density functional theory (DFT), as implemented in the SIESTA code.⁵⁹ The exchange-correlation term is given in the generalized gradient approximation (GGA-PBE).⁶⁰ The wave functions are described as a linear combination of atomic orbitals with a sum of z-basis set with polarized function (DZP).⁵⁹ The norm-conserving Troullier-Martins pseudopotential (with a Bylander factorized form) is used to represent the interaction between valence electrons and atomic ions.^{61,62}

The reciprocal space is sampled on a Monkhorst-Pack scheme with a $2 \times 2 \times 2$ k-point mesh.⁶³ The calculations were performed with a mesh cut-off of 200 Ry considering that the Brillouin zone is sampled by k-points along with a simple cubic cell.

We considered that each self-consistent calculation cycle is performed until the convergence is achieved when the maximum difference between elements of the density matrix is smaller than 10^{-4} eV. In the structural optimization procedure, we let the atoms and lattice parameters vary until the convergence is achieved when the force on each atom was less than 0.01 eVÅ.

Then we computed the formation energy for each schwarzite structure composed of germanium atoms and for comparison purposes, we also considered germanene and germanium at fcc unit-cell (diamond structure).

In order to investigate if occur appreciable structural changes at room temperature, we performed ab initio molecular dynamics (AIMD) simulations using the siesta code at $T = 300$ K. We used a time step of 0.1 fs in an NVT ensemble for a total simulation time of 2 ps. For control the temperature in the AIMD simulations we employed the Nos-Hoover thermostat.

From the optimized structures, we performed optical calculations using the same parameters earlier discussed (used in siesta code). The optical properties were obtained assuming that an external electric field of magnitude 1.0 V/\AA is polarized as a medium of the three spatial directions.

Trough the complex dielectric function $\epsilon = \epsilon_1 + i\epsilon_2$, were determined all relevant optical properties, where ϵ_1 and ϵ_2 are real and imaginary, respectively.

From Kramers-Kronig transformation, is possible to derive ϵ_1 as

$$\epsilon_1(\omega) = 1 + \frac{1}{\pi} P \int_0^\infty d\omega' \frac{\omega' \epsilon_2(\omega')}{\omega'^2 - \omega^2}, \quad (1)$$

where ω is the frequency of photon.

From Fermi's golden rule, its possible to show that the imaginary part, ϵ_2 , is given by:

$$\epsilon_2(\omega) = \frac{4\pi^2}{\Omega\omega^2} \sum_{i \in \text{VB}, j \in \text{CB}} \sum_k W_k |\rho_{ij}|^2 \delta(\epsilon_{kj} - \epsilon_{ki} - \omega), \quad (2)$$

where VB and CB denotes the valence and conduction band, respectively, Ω is the unit cell volume and ρ_{ij} is the dipole transition matrix element.

Once the part real and imaginary of dielectric function were determined, the absorption coefficient α , reflectivity R and refractive index η , are determined directly by expressions:

$$\alpha(\omega) = \sqrt{2}\omega \left[(\epsilon_1^2(\omega) + \epsilon_2^2(\omega))^{1/2} - \epsilon_1(\omega) \right]^{1/2}, \quad (3)$$

$$R(\omega) = \left[\frac{(\epsilon_1(\omega) + i\epsilon_2(\omega))^{1/2} - 1}{(\epsilon_1(\omega) + i\epsilon_2(\omega))^{1/2} + 1} \right]^2, \quad (4)$$

$$\eta(\omega) = \frac{1}{\sqrt{2}} \left[(\epsilon_1^2(\omega) + \epsilon_2^2(\omega))^{1/2} + \epsilon_1(\omega) \right]^2. \quad (5)$$

Results and discussion

Structural stability at $T = 0$ K

In Figure 1 we present the optimized germanium-based schwarzite structures. All structures are stable at $T = 0$ K. D688, G688 and P8bal contain 24, 96 and 192 atoms in their unit cell, respectively. The obtained structural shapes are very similar to the ones of carbon-based

schwarzites, with the exception of the buckling (see inset of figure 1-c)), which becomes more pronounced as the structures contain larger flat segments and is a consequence of the pseudo-Jahn-Teller effect.^{56,57} Another difference is the typical bond length values, which are ~ 2.4 Å for germanium in comparison to ~ 1.5 Å for carbon.⁶⁴

We also calculated the formation energy of the schwarzites and compared them to the corresponding values of germanene (already synthesized) and germanium (diamond structure) calculated using the same computational approach. The formation energy values were obtained using the following expression:

$$E_f = \frac{E_{\text{structure}} - N_{\text{Ge}}E_{\text{Ge}}}{N_{\text{Ge}}}, \quad (6)$$

where $E_{\text{structure}}$ is the total energy of the structure, E_{Ge} is the total energy of one isolated germanium atom and N_{Ge} is the number of germanium atoms present in each structure. We calculated the total energy of a germanium atom considering it placed within a large simulation box.

The results are presented in Table 1. We can see that the energies for schwarzites are not very high in comparison to other structures occurring in nature or/and that were previously synthesized. This is indicative of their synthesis feasibility.

Table 1: Formation energies of germanium-based schwarzites, germanene, and germanium (fcc).

Structure	E_f (eV/atom)
D688	-4.25
G688	-4.39
P8bal	-4.30
Germanium (fcc)	-4.63
Germanene	-4.40

In order to verify whether significant structural changes occur at room temperature, we also performed AIMD with a NVT ensemble during 2 ps at $T = 300$ K.

In Figure 2 we present snapshots of the obtained equilibrated structures after 2 ps AIMD

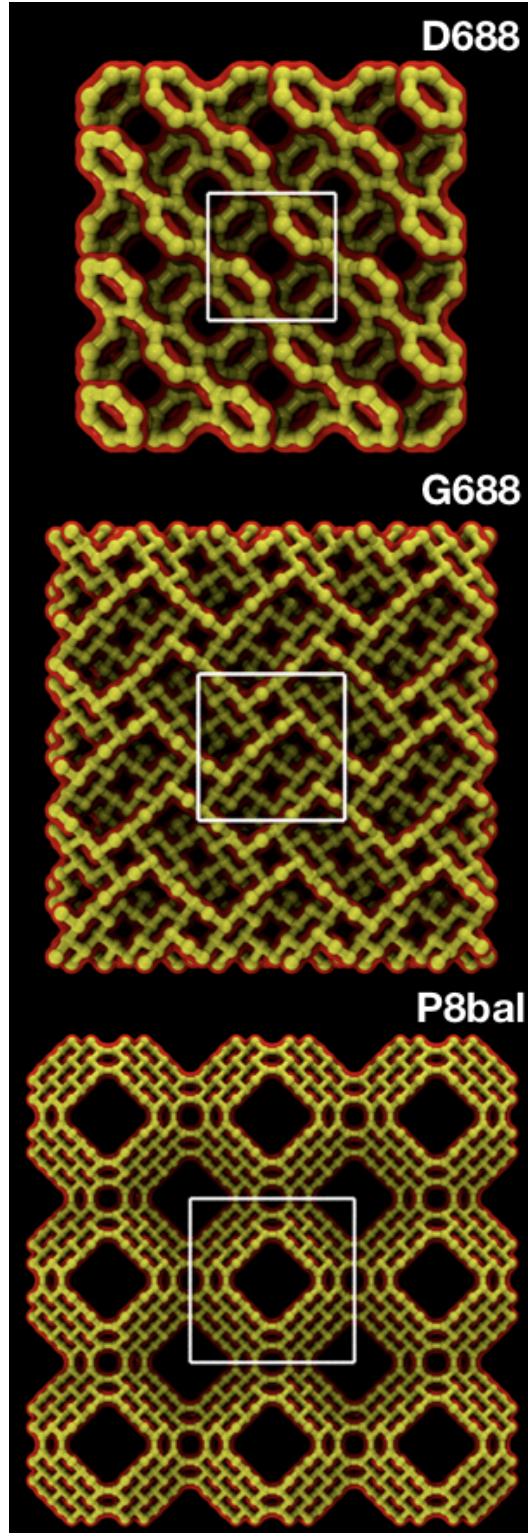


Figure 1: Optimized structures of germanium-based schwarzites with square unit cell highlighted replicated $2 \times 2 \times 2$: a) D688, b) G688 and c) P8bal. In the inset of figure 1-c) we can see the observed pronounced buckling.

simulations. When the thermostat is set on, the shape of structures remained similar to those obtained at $T = 0$ K and showed in the figure 1. There are only small structural differences between the two cases, which can be attributed to thermal fluctuations. These results indicate that the structures are stable at room temperature and do not exhibit significant thermal induced structural changes.

Electronic Analysis

In Figure 3 we present the calculated electronic band structures and their corresponding projected total density of states (PDOS) for the schwarzites shown in 1. The displayed band structures used the same special k-points from reference.⁶⁴

From Figure 3 we can see that only the D688 presents a metallic behavior, the valence/conduction bands touch at R symmetry point. The structures G688 and P8bal are semiconductors with a small direct gap at Γ point with values of 0.27 and 0.13 eV, respectively.

It is interesting to notice that although carbon and germanium are in the same IV group and the schwarzite structures are quite similar (with the exception of a more pronounced buckling in the case of germanium), their electronic structures are quite different, especially with relation to the bandgap values. Carbon-based D66, G688 and P8bal schwarzites present bandgap values of 2.9, 1.5, 1.4 eV, respectively,²⁵ i. e., much larger values than the corresponding germanium structures.

In Figure 4 we show the highest occupied crystal orbital (HOCO) and lowest-unoccupied crystal orbital (LUCO) of the schwarzites shown in 1. We can see from this Fig. that the HOCO and LUCO are well delocalized for all structures.

Optical Analysis

In Fig. 5 we present the optical coefficients results as a function of photon energy value. The light is polarized as the average of x , y and z directions. In the Fig. 5-a), we present

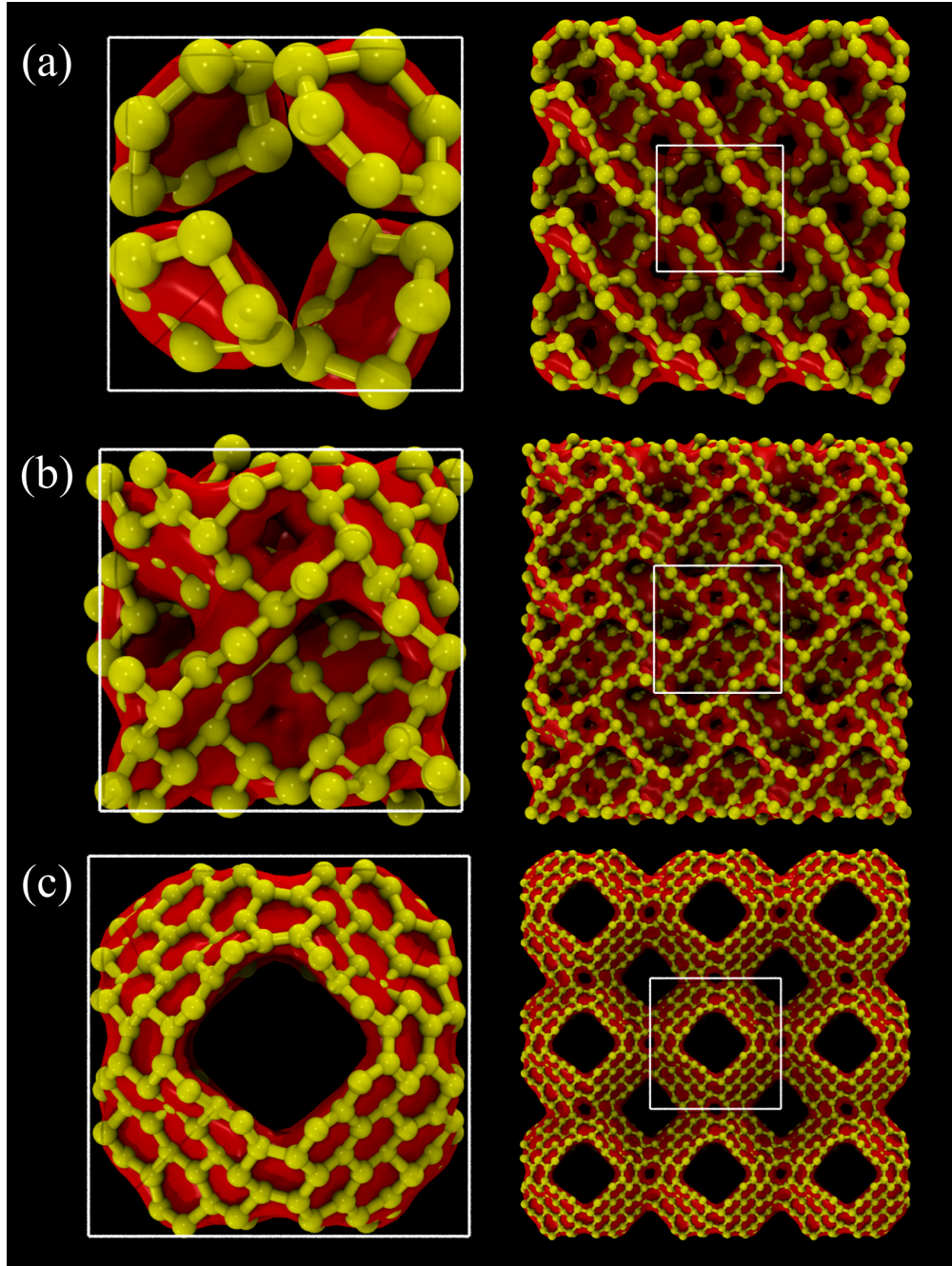


Figure 2: Snapshots of the obtained equilibrated structures after 2 ps AIMD simulations. (a) D688; (b) G688; and (c) P8bal. Left and right correspond to the used unit cells and their replicated ($3 \times 3 \times 3$) supercells, respectively.

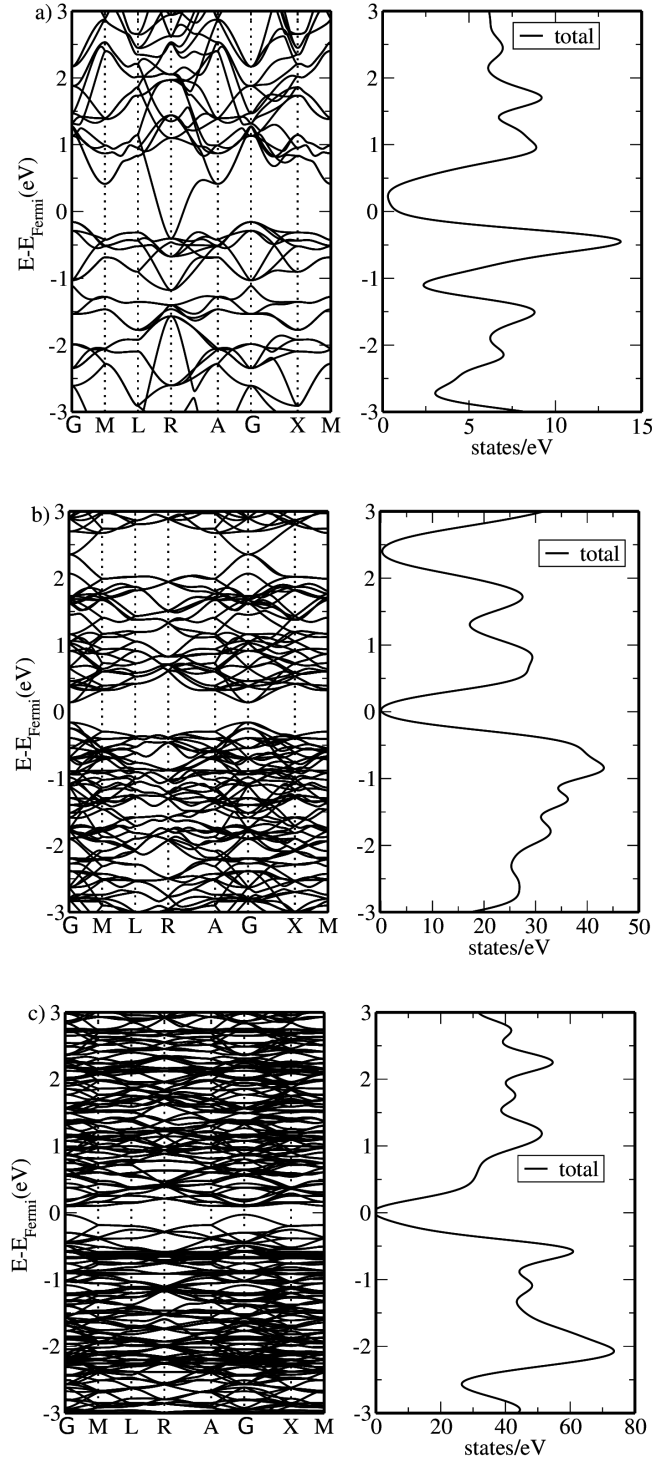


Figure 3: Calculated electronic band structures and their corresponding projected total density of states for the schwarzites shown in 1. The Fermi level value is set to zero.

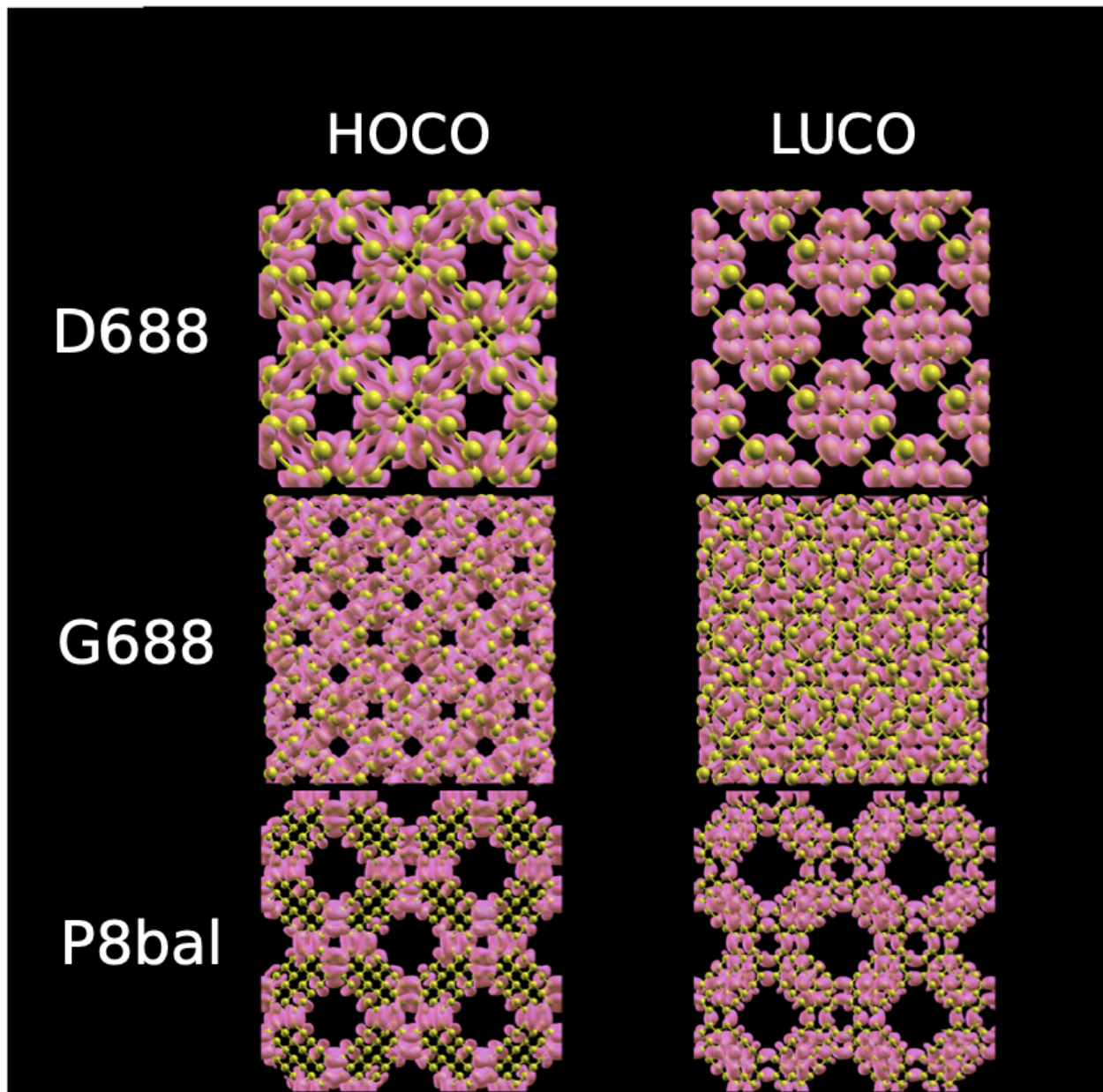


Figure 4: HOCO (left) and LUCO (right) of the schwarzites shown in Fig. 1.

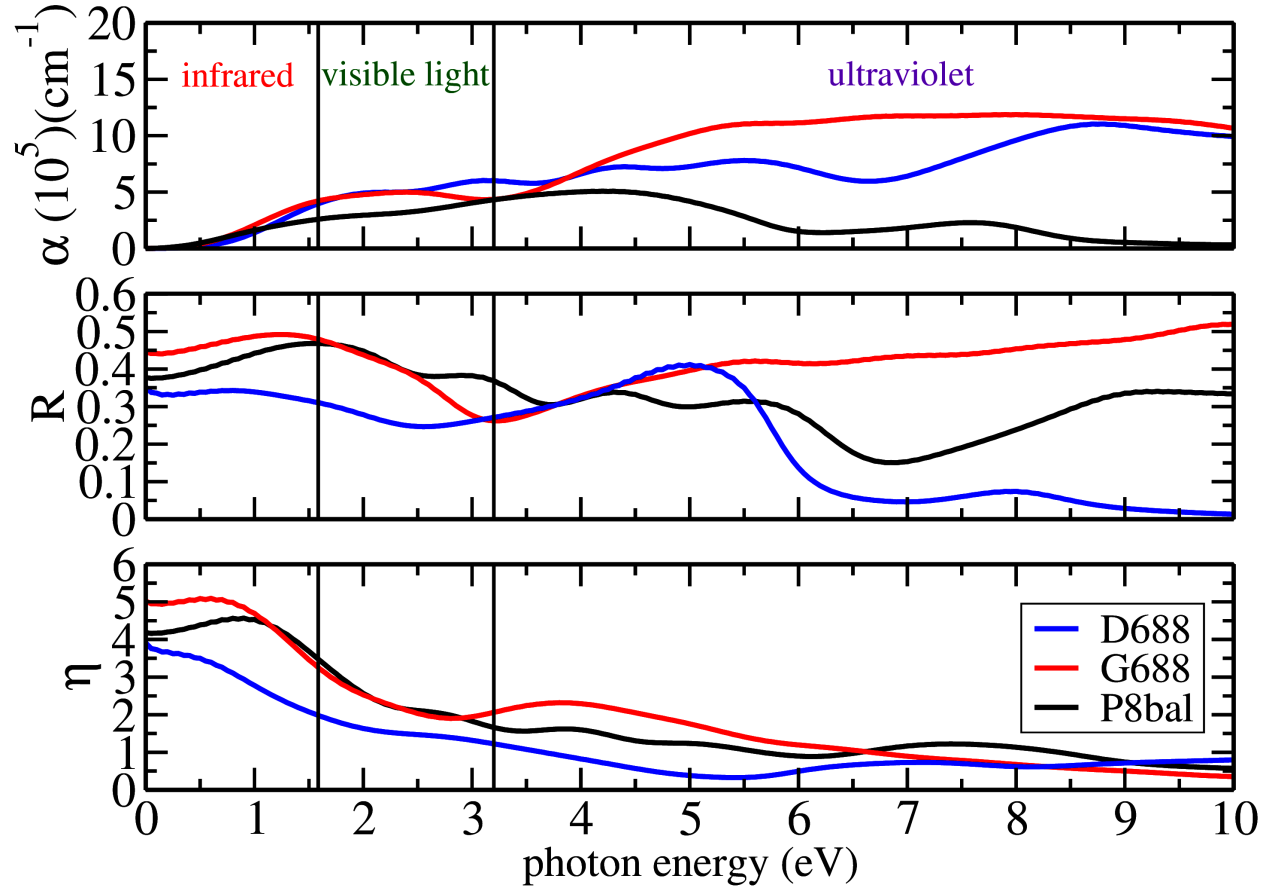


Figure 5: From top to bottom: (a) absorption coefficient; (b) reflectivity; and (c) refractivity index as a function of photon energy for schwarzites shown in Fig. 1.

the absorption coefficients results. The absorption starts in the infrared region near zero for all cases. This is expected because D688 is metallic and G688 and P8bal are semiconductors with small direct bandgap values (0.27 and 0.13 eV, respectively at Γ point). These bandgaps are associated with the first optical transition between HOCO to LUCO. The analyses of the PDOS (3) show that these transitions involve bonding ($p_{x,y,z}, \pi$) orbitals to anti-bonding ($p_{x,y,z}, \pi^*$) ones. There is no preferential polarization axis because of the spatial orbital symmetries.

We noticed that all germanium-based schwarzite structures have a small optical activity in infrared region. The same behavior was observed for germanene,⁶⁵ germanium (diamond)⁶⁶ and germanium-doped graphene structures.⁶⁷ The structures have almost the same behavior in the infrared regions and become more differentiated for the visible and ultraviolet regions.

In Fig. 5-b and c we present the results for reflectivity and refractivity, respectively. All structures exhibit good reflectivity in the infrared, visible and ultraviolet (with the exception of D688). The corresponding refractivity continuously decreases from infrared to ultraviolet regions. Therefore the major part of the incident light will be absorbed and a small quantity will be reflected. This is indicative that the structures could be good candidates for solar cell applications, ultraviolet blocks and/or other optoelectronic devices.

Mechanical Properties

In Fig. 6-top) we present the strain-stress curves for the structures shown in Fig. 1 considering an applied uniaxial tensile deformation along the x-crystal axis. The Young's modulus values can be estimated from the linear region of the curves. The obtained values are 20, 22 and 11 GPa for D688, G688, and P8bal, respectively. These values are typically one order of magnitude lower than the corresponding carbon-based structures (139, 156, and 67¹¹), but preserved the ordering values.

The structures D688 and P8bal exhibit similar trends in the stress-strain curves, while G688 a quite different one. This can be explained by the different deformation mechanisms.

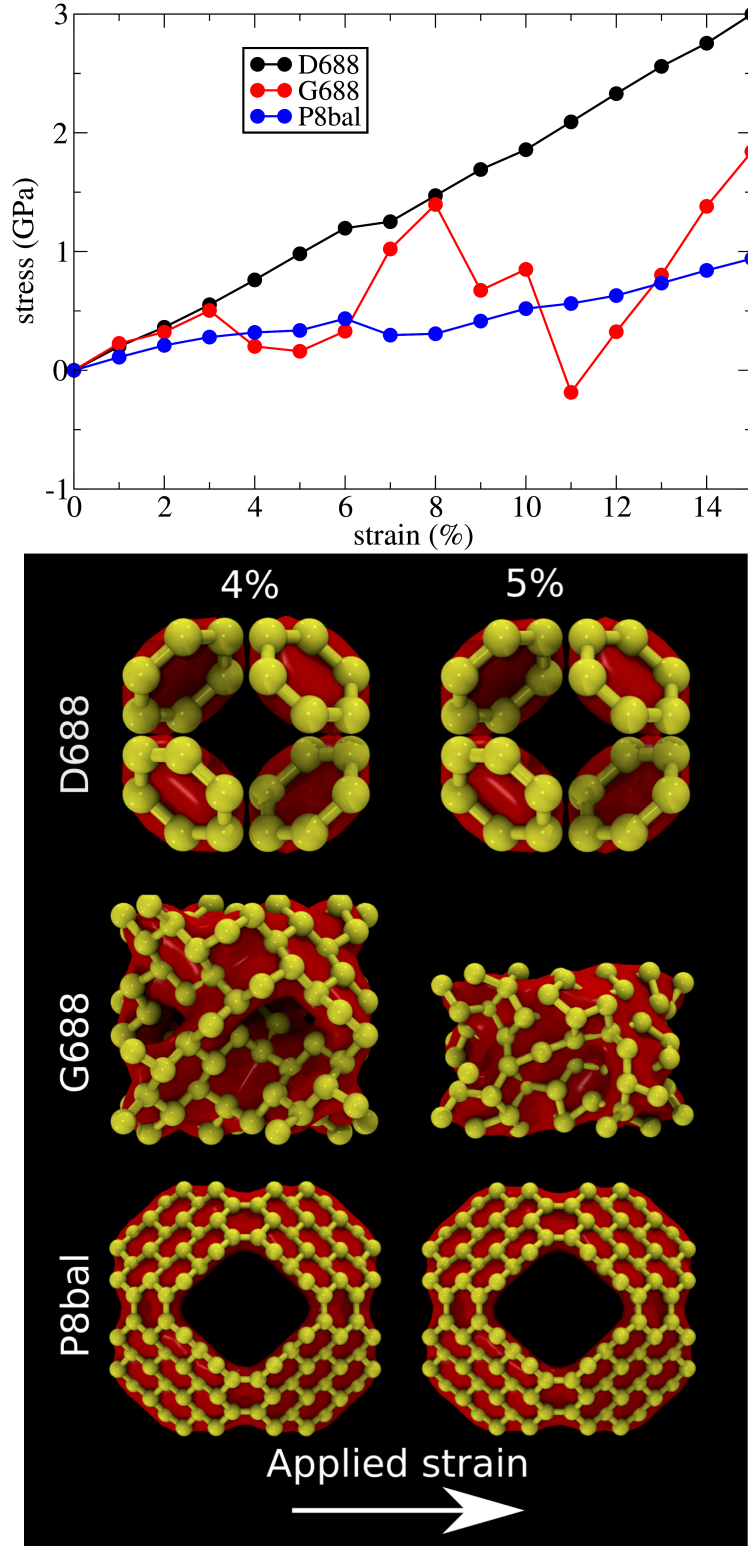


Figure 6: Top: stress x strain curves for the structures shown in Fig. 1; Bottom: representative snapshots of the deformed structures at 4 and 5%, respectively.

In the bottom part of the Fig. 6 we present representative snapshots of the deformed structures. As the schwarzites are very porous and elastic structures, a nature deformation mechanism is 'pore' closing,^{10,12,68,69} which are present for all structures shown in Fig. 6. But only G668 exhibits a pore collapse (indicated the abrupt drops in the stress-strain curves. The whole process can be better understood from the videos1-3 in the Supplementary Materials. This behavior was also reported for other carbon-based schwarzites.¹²

Summary and Conclusions

In summary, we have investigated using first-principles methods (SIESTA) the structural stability, mechanical and optical properties of different families of germanium-based schwarzites.

Our results show that all structures are stable and with formation energy values compatibles with other previously synthesized germanium allotropes (such as germanenes). The obtained optimized structures are structurally very similar to the ones reported to carbon-based schwarzites. Results from *ab initio* molecular dynamics simulations at $T = 300$ K, do not indicate significant thermal structural changes.

Germanium-based schwarzites can be metallic (D688) or small bandgap semiconductors (0.27 and 0.13 eV for G688 and P8bal structures, respectively).

They can absorb light in a large spectrum, from infrared to ultraviolet and with average reflectivity around about 40-50% and refractivity index about 2-3 in the visible region. These results suggest that these structures can be good candidates for building optoelectronics devices, solar cell applications, and ultraviolet blockers.

One important issue is the synthesis feasibility of these structures. The schwarzite synthesis has been elusive, but there are recent important synthesis advances exploiting zeolite as templates.⁶⁻⁸ It is expected that schwarzite large-size fragments could be a reality in the coming years. We hope the present study can stimulate further studies on these remarkable germanium allotrope structures.

Acknowledgements

This work was financed in part by the Coordenao de Aperfeioamento de Pessoal de Nvel Superior - Brasil (CAPES) - Finance Code 001 and CNPq and FAPESP. The authors thank the Center for Computational Engineering and Sciences at Unicamp for financial support through the FAPESP/CEPID Grant #2013/08293-7.

References

- (1) Mackay, A. L.; Terrones, H. Diamond from graphite. *Nature* **1991**, *352*, 762–762.
- (2) Terrones, H.; Mackay, A. The geometry of hypothetical curved graphite structures. *Carbon* **1992**, *30*, 1251–1260.
- (3) O’Keeffe, M.; Adams, G.; Sankey, O. Predicted new low energy forms of carbon. *Physical Review Letters* **1992**, *68*, 2325–2328.
- (4) Terrones, H.; Mackay, A. From C60 to negatively curved graphite. *Progress in Crystal Growth and Characterization of Materials* **1997**, *34*, 25–36.
- (5) Vanderbilt, D.; Tersoff, J. Negative-curvature fullerene analog of C60. *Physical Review Letters* **1992**, *68*, 511–513.
- (6) Nishihara, H.; Yang, Q.-H.; Hou, P.-X.; Unno, M.; Yamauchi, S.; Saito, R.; Paredes, J. I.; Martnez-Alonso, A.; Tascn, J. M.; Sato, Y.; Terauchi, M.; Kyotani, T. A possible buckybowl-like structure of zeolite templated carbon. *Carbon* **2009**, *47*, 1220–1230.
- (7) Nishihara, H.; Kyotani, T. Zeolite-templated carbons - three-dimensional microporous graphene frameworks. *Chemical Communications* **2018**, *54*, 5648–5673.
- (8) Braun, E.; Lee, Y.; Moosavi, S. M.; Barthel, S.; Mercado, R.; Baburin, I. A.; Proserpio, D. M.; Smit, B. Generating carbon schwarzites via zeolite-templating. *Proceedings*

- of the National Academy of Sciences of the United States of America* **2018**, *115*, E8116–E8124.
- (9) Farrell, J. M.; Grande, V.; Schmidt, D.; Wrthner, F. A Highly Warped HeptagonContaining sp² Carbon Scaffold via Vinylaphthyl π Extension. *Angewandte Chemie* **2019**, *131*, 16656–16656.
 - (10) Sajadi, S. M.; Owuor, P. S.; Schara, S.; Woellner, C. F.; Rodrigues, V.; Vajtai, R.; Lou, J.; Galvo, D. S.; Tiwary, C. S.; Ajayan, P. M. Multiscale geometric design principles applied to 3D printed schwarzites. *Advanced Materials* **2018**, *30*.
 - (11) Miller, D. C.; Terrones, M.; Terrones, H. Mechanical properties of hypothetical graphene foams: Giant Schwarzites. *Carbon* **2016**, *96*, 1191–1199.
 - (12) Felix, L. C.; Woellner, C. F.; Galvao, D. S. Mechanical and energy-absorption properties of schwarzites. *Carbon* **2019**, *157*, 670–680.
 - (13) Jung, G. S.; Buehler, M. J. Multiscale Mechanics of Triply Periodic Minimal Surfaces of Three-Dimensional Graphene Foams. *Nano Letters* **2018**, *18*, 4845–4853.
 - (14) Pedrielli, A.; Taioli, S.; Garberoglio, G.; Pugno, N. M. Designing graphene based nanofoams with nonlinear auxetic and anisotropic mechanical properties under tension or compression. *Carbon* **2017**, *111*, 796–806.
 - (15) Lu, W.; Chung, D. D. L. Mesoporous activated carbon filaments. *MRS Proceedings* **1996**, *454*, 9.
 - (16) Kyotani, T. Control of pore structure in carbon. *Carbon* **2000**, *38*, 269–286.
 - (17) Damasceno Borges, D.; Galvao, D. S. Schwarzites for Natural Gas Storage: A Grand-Canonical Monte Carlo Study. *MRS Advances* **2018**, *3*, 115–120.

- (18) Collins, S. P.; Perim, E.; Daff, T. D.; Skaf, M. S.; Galvão, D. S.; Woo, T. K. Idealized Carbon-Based Materials Exhibiting Record Deliverable Capacities for Vehicular Methane Storage. *Journal of Physical Chemistry C* **2019**, *123*, 1050–1058.
- (19) Park, S.; Kittimanapun, K.; Ahn, J. S.; Kwon, Y.-K.; Tomnek, D. Designing rigid carbon foams. *Journal of Physics. Condensed Matter* **2010**, *22*, 334220.
- (20) Odkhuu, D.; Jung, D. H.; Lee, H.; Han, S. S.; Choi, S.-H.; Ruoff, R. S.; Park, N. Negatively curved carbon as the anode for lithium ion batteries. *Carbon* **2014**, *66*, 39–47.
- (21) Barborini, E.; Piseri, P.; Milani, P.; Benedek, G.; Ducati, C.; Robertson, J. Negatively curved spongy carbon. *Applied physics letters* **2002**, *81*, 3359–3361.
- (22) Benedek, G.; Vahedi-Tafreshi, H.; Barborini, E.; Piseri, P.; Milani, P.; Ducati, C.; Robertson, J. The structure of negatively curved spongy carbon. *Diamond and related materials* **2003**, *12*, 768–773.
- (23) Wu, Y. et al. Three-dimensionally bonded spongy graphene material with super compressive elasticity and near-zero Poisson’s ratio. *Nature Communications* **2015**, *6*, 6141.
- (24) Townsend, S.; Lenosky, T.; Muller, D.; Nichols, C.; Elser, V. Negatively curved graphitic sheet model of amorphous carbon. *Physical Review Letters* **1992**, *69*, 921–924.
- (25) Valencia, F.; Romero, A. H.; Hernandez, E.; Terrones, M.; Terrones, H. Theoretical characterization of several models of nanoporous carbon. *New journal of physics* **2003**, *5*, 123–123.
- (26) Phillips, R.; Drabold, D. A.; Lenosky, T.; Adams, G. B.; Sankey, O. F. Electronic structure of schwarzite. *Physical Review B* **1992**, *46*, 1941–1943.
- (27) Gaito, S.; Colombo, L.; Benedek, G. A theoretical study of the smallest tetrahedral carbon schwarzites. *Europhysics Letters (EPL)* **1998**, *44*, 525–530.

- (28) Huang, M.-Z.; Ching, W. Y.; Lenosky, T. Electronic properties of negative-curvature periodic graphitic carbon surfaces. *Physical Review B* **1993**, *47*, 1593–1606.
- (29) Tagami, M.; Liang, Y.; Naito, H.; Kawazoe, Y.; Kotani, M. Negatively curved cubic carbon crystals with octahedral symmetry. *Carbon* **2014**, *76*, 266–274.
- (30) Weng, H.; Liang, Y.; Xu, Q.; Yu, R.; Fang, Z.; Dai, X.; Kawazoe, Y. Topological node-line semimetal in three-dimensional graphene networks. *Physical Review B* **2015**, *92*, 045108.
- (31) Park, N.; Yoon, M.; Berber, S.; Ihm, J.; Osawa, E.; Tomnek, D. Magnetism in all-carbon nanostructures with negative Gaussian curvature. *Physical Review Letters* **2003**, *91*, 237204.
- (32) Zhang, Z.; Chen, J.; Li, B. Negative Gaussian curvature induces significant suppression of thermal conduction in carbon crystals. *Nanoscale* **2017**, *9*, 14208–14214.
- (33) Pereira, L. F. C.; Savi, I.; Donadio, D. Thermal conductivity of one-, two- and three-dimensional sp² carbon. *New journal of physics* **2013**, *15*, 105019.
- (34) Zhang, Z.; Hu, S.; Nakayama, T.; Chen, J.; Li, B. Reducing lattice thermal conductivity in schwarzites via engineering the hybridized phonon modes. *Carbon* **2018**, *139*, 289–298.
- (35) Gao, P.; Chen, X.; Guo, L.; Wu, Z.; Zhang, E.; Gong, B.; Zhang, Y.; Zhang, S. BN-schwarzite: novel boron nitride spongy crystals. *Physical Chemistry Chemical Physics* **2017**, *19*, 1167–1173.
- (36) LaViolette, R. A.; Benson, M. T. Density functional calculations of hypothetical neutral hollow octahedral molecules with a 48-atom framework: Hydrides and oxides of boron, carbon, nitrogen, aluminum, and silicon. *The Journal of Chemical Physics* **2000**, *112*, 9269–9275.

- (37) Zhang, F.; Stojkovic, D. S.; Crespi, V. H. Theory of a three-dimensional nanoporous silicon lattice with unsaturated bonding. *Applied physics letters* **2010**, *97*, 121906.
- (38) Rthlisberger, U.; Andreoni, W.; Parrinello, M. Structure of nanoscale silicon clusters. *Physical Review Letters* **1994**, *72*, 665–668.
- (39) Zhang, R.; Lee, S.; Law, C.-K.; Li, W.-K.; Teo, B. K. Silicon nanotubes: Why not? *Chemical physics letters* **2002**, *364*, 251–258.
- (40) Durgun, E.; Tongay, S.; Ciraci, S. Silicon and III-V compound nanotubes: Structural and electronic properties. *Physical Review B* **2005**, *72*, 075420.
- (41) Bai, J.; Zeng, X. C.; Tanaka, H.; Zeng, J. Y. Metallic single-walled silicon nanotubes. *Proceedings of the National Academy of Sciences of the United States of America* **2004**, *101*, 2664–2668.
- (42) Guo, L.; Zheng, X.; Liu, C.; Zhou, W.; Zeng, Z. An ab initio study of cluster-assembled hydrogenated silicon nanotubes. *Computational and Theoretical Chemistry* **2012**, *982*, 17–24.
- (43) Fagan, S. B.; Baierle, R. J.; Mota, R.; da Silva, A. J. R.; Fazzio, A. Ab initio calculations for a hypothetical material: Silicon nanotubes. *Physical Review B* **2000**, *61*, 9994–9996.
- (44) Singh, A. K.; Kumar, V.; Kawazoe, Y. Metal encapsulated nanotubes of silicon and germanium. *J. Mater. Chem.* **2004**, *14*, 555.
- (45) Takeda, K.; Shiraishi, K. Theoretical possibility of stage corrugation in Si and Ge analogs of graphite. *Physical review. B, Condensed matter* **1994**, *50*, 14916–14922.
- (46) Cahangirov, S.; Topsakal, M.; Aktrk, E.; Sahin, H.; Ciraci, S. Two- and one-dimensional honeycomb structures of silicon and germanium. *Physical Review Letters* **2009**, *102*, 236804.

- (47) Topsakal, M.; Ciraci, S. Elastic and plastic deformation of graphene, silicene, and boron nitride honeycomb nanoribbons under uniaxial tension: A first-principles density-functional theory study. *Physical Review B* **2010**, *81*, 024107.
- (48) Zhao, H. Strain and chirality effects on the mechanical and electronic properties of silicene and silicane under uniaxial tension. *Physics Letters A* **2012**, *376*, 3546–3550.
- (49) Botari, T.; Perim, E.; Autreto, P. A. S.; van Duin, A. C. T.; Paupitz, R.; Galvao, D. S. Mechanical properties and fracture dynamics of silicene membranes. *Physical Chemistry Chemical Physics* **2014**, *16*, 19417–19423.
- (50) Ni, Z.; Liu, Q.; Tang, K.; Zheng, J.; Zhou, J.; Qin, R.; Gao, Z.; Yu, D.; Lu, J. Tunable bandgap in silicene and germanene. *Nano Letters* **2012**, *12*, 113–118.
- (51) O’Hare, A.; Kusmartsev, F. V.; Kugel, K. I. A stable ”flat” form of two-dimensional crystals: could graphene, silicene, germanene be minigap semiconductors? *Nano Letters* **2012**, *12*, 1045–1052.
- (52) Vogt, P.; De Padova, P.; Quaresima, C.; Avila, J.; Frantzeskakis, E.; Asensio, M. C.; Resta, A.; Ealet, B.; Le Lay, G. Silicene: compelling experimental evidence for graphenelike two-dimensional silicon. *Physical Review Letters* **2012**, *108*, 155501.
- (53) Dvila, M. E.; Xian, L.; Cahangirov, S.; Rubio, A.; Le Lay, G. Germanene: a novel two-dimensional germanium allotrope akin to graphene and silicene. *New journal of physics* **2014**, *16*, 095002.
- (54) Vogt, P.; Capiod, P.; Berthe, M.; Resta, A.; De Padova, P.; Bruhn, T.; Le Lay, G.; Grandidier, B. Synthesis and electrical conductivity of multilayer silicene. *Applied physics letters* **2014**, *104*, 021602.
- (55) De Padova, P.; Ottaviani, C.; Quaresima, C.; Olivieri, B.; Imperatori, P.; Salomon, E.; Angot, T.; Quagliano, L.; Romano, C.; Vona, A.; Muniz-Miranda, M.; Generosi, A.;

- Paci, B.; Le Lay, G. 24 h stability of thick multilayer silicene in air. *2D Materials* **2014**, *1*, 021003.
- (56) Bersuker, I. B. Pseudo-Jahn-teller effect—a two-state paradigm in formation, deformation, and transformation of molecular systems and solids. *Chemical Reviews* **2013**, *113*, 1351–1390.
- (57) Hobey, W. D. Vibronic interaction of nearly degenerate states in substituted benzene anions. *The Journal of Chemical Physics* **1965**, *43*, 2187–2199.
- (58) Perim, E.; Paupitz, R.; Botari, T.; Galvao, D. S. One-dimensional silicon and germanium nanostructures with no carbon analogues. *Physical Chemistry Chemical Physics* **2014**, *16*, 24570–24574.
- (59) Soler, J. M.; Artacho, E.; Gale, J. D.; García, A.; Junquera, J.; Ordejón, P.; Sánchez-Portal, D. The SIESTA method for ab initio order-N materials simulation. *J. Phys. Condens. Matter* **2002**, *14*, 2745.
- (60) Perdew, J. P.; Burke, K.; Ernzerhof, M. Generalized gradient approximation made simple. *Phys. Rev. Lett.* **1996**, *77*, 3865.
- (61) Troullier, N.; Martins, J. L. Efficient pseudopotentials for plane-wave calculations. *Phys. Rev. B* **1991**, *43*, 1993–2006.
- (62) Kleinman, L.; Bylander, D. M. Efficacious Form for Model Pseudopotentials. *Phys. Rev. Lett.* **1982**, *48*, 1425–1428.
- (63) Monkhorst, H. J.; Pack, J. D. Special points for Brillouin-zone integrations. *Phys. Rev. B* **1976**, *13*, 5188.
- (64) Feng, X.; Mu, H.; Xiang, Z.; Cai, Y. Theoretical investigation of negatively curved 6.82D carbon based on density functional theory. *Computational Materials Science* **2020**, *171*, 109211.

- (65) John, R.; Merlin, B. Optical properties of graphene, silicene, germanene, and stanene from IR to far UV A first principles study. *Journal of Physics and Chemistry of Solids* **2017**, *110*, 307 – 315.
- (66) Goh, E. S. M.; Chen, T. P.; Sun, C. Q.; Liu, Y. C. Thickness effect on the band gap and optical properties of germanium thin films. *Journal of Applied Physics* **2010**, *107*, 24305.
- (67) Ould Ne, M. L.; Abbassi, A.; El hachimi, A. G.; Benyoussef, A.; Ez-Zahraouy, H.; El Kenz, A. Electronic optical, properties and widening band gap of graphene with Ge doping. *Optical and Quantum Electronics* **2017**, *49*, 218.
- (68) Woellner, C. F.; Botari, T.; Perim, E.; Galvo, D. S. Mechanical Properties of Schwarzites - A Fully Atomistic Reactive Molecular Dynamics Investigation. *MRS Advances* **2018**, *3*, 451–456.
- (69) Felix, L. C.; Gal, V.; Woellner, C. F.; Rodrigues, V.; Galvao, D. S. Mechanical Properties of Diamond Schwarzites: From Atomistic Models to 3D-Printed Structures. *MRS Advances* **2020**, 1–7.

Graphical TOC Entry

Some journals require a graphical entry for the Table of Contents. This should be laid out "print ready" so that the sizing of the text is correct. Inside the `tocentry` environment, the font used is Helvetica 8 pt, as required by *Journal of the American Chemical Society*. The surrounding frame is 9 cm by 3.5 cm, which is the maximum permitted for *Journal of the American Chemical Society* graphical table of content entries. The box will not resize if the content is too big: instead it will overflow the edge of the box. This box and the associated title will always be printed on a separate page at the end of the document.